

Conformation of an octapeptide fragment (2-9) of kaliocin-1 in DMSO-d₆ by ¹H NMR and restrained molecular dynamics

P N Sunilkumar¹, C Sadasivan², K S Devaky³ and M Haridas^{2*}

¹School of Biosciences, Mahatma Gandhi University, Kottayam, Kerala 686 560, India

²Department of Biotechnology and Microbiology, School of Life Sciences, Kannur University, Thalassery Campus, Palayad P.O., Kerala 670 661, India

³School of Chemical Sciences, Mahatma Gandhi University, Kottayam, Kerala 686 560, India

Received 3 August 2006; revised 20 January 2007

Kaliocin-1, a 31-residue synthetic peptide (FFSASCVPGADKQGFPNLCRLCA GTGENKCA), which has shown the antimicrobial activity forms the 152-182 fragment of human lactoferrin (HLf). As the octapeptide FSASCVPG forms the 2-9 fragment of kaliocin-1, in the present study, its conformation in dimethyl sulfoxide-d₆ (DMSO-d₆) has been determined using two-dimensional (2D) nuclear magnetic resonance (NMR) spectroscopy as well as restrained molecular dynamics. Sequence specific assignments of all the ¹H resonances have been carried out using 2D correlation experiments (2D DQF-COSY, TOCSY and ROESY). In dimethyl sulfoxide-d₆ at 25°C, the octapeptide adopts a predominantly extended backbone conformation. The calculated structure resembles closely with the reported structure of the corresponding fragment of HLf. The peptide also has sequence and structural similarity with the corresponding fragments of lactoferrins from other organisms.

Keywords: Kaliocin-1, Nuclear magnetic resonance, Peptide conformation, Dimethyl sulfoxide-d₆, Restrained molecular dynamics.

The octapeptide FSASCVPG forms the 153-160 fragment of human lactoferrin (HLf), a protein having 691 residues¹. Kaliocin-1, a 31-residue synthetic peptide (FFSASCVPGADKQGFPNLCRLCAGTGENKCA) has shown antimicrobial effect² and forms the 152-182 fragment of HLf¹. The octapeptide FSASCVPG, which is the focus of the present study, forms the 2-9 fragment of kaliocin-1 also². The

antimicrobial activity of kaliocin-1 is lower than that of HLf, but Na⁺ or K⁺ inhibit their activities in a concentration-dependent manner². Kaliocin-1 has been found to mimic native lactoferrin, inducing K⁺-efflux and a selective dissipation of the transmembrane electrical potential of *E. coli* cells without causing extensive damage to the outer and inner bacterial membranes². Kaliocin-1, but not lactoferrin, has been found to permeabilize different ions through liposomal membranes². It is not cytotoxic and can be used as a suitable model for the design of analogs that are able to mimic the antimicrobial activity of HLf.

Interestingly, kaliocin-1 sequence is homologous to other sequences present in the N- and C-terminal lobes of all members of transferrin family proteins². Sequences homologous to kaliocin-1 sequence in transferrins may be involved in the well-known antimicrobial activities of these evolutionarily ancient proteins². The sequence of kaliocin-1 includes the amino acid sequence of the N-terminal region of HLf². The octapeptide sequence FSASCVPG shows around 87.5% conservation with the corresponding fragments in lactoferrins from different organisms such as murine (MLf), goat (GLf), bovine (CLf), and

*For correspondence:

Email: mharidasm@rediffmail.com

Tel: +91 0490 2347394; Fax: +91 0490 2345317

Abbreviations: APSSP, advanced protein secondary structure prediction; BLf, buffalo lactoferrin; BDDMA-PS, 1, 4-butanediol dimethacrylate cross-linked polystyrene; Boc, tert-butyloxy carbonyl; CLf, bovine lactoferrin; CSI, chemical shift index; 2D, two-dimensional; 3D, three-dimensional; DCC, dicyclohexyl carbodiimide; DMSO-d₆, dimethyl sulfoxide-d₆; DQF-COSY, double quantum filtered correlation spectroscopy; EDT, ethanedithiol; FT, fourier transform; GLf, goat lactoferrin; HLf, human lactoferrin; HOBt, 1-hydroxybenzotriazole; MLf, murine lactoferrin; NMR, nuclear magnetic resonance; NOE, nuclear overhauser enhancement; NOESY, nuclear overhauser enhancement spectroscopy; PLf, porcine lactoferrin; RMSD, root mean square deviation; ROESY, rotating-frame overhauser enhancement spectroscopy; TAD, torsional angle dynamics; TFA, trifluoroacetic acid; TOCSY, total correlation spectroscopy; TSP, 3-(trimethylsilyl) [3,3,2,2-²H]propionate-d₄. Standard abbreviations of amino acids were used.

buffalo (BLf) and 75% conservation with that from porcine lactoferrin (PLf)³ (Fig. 1) and with the 489-496 fragment in the C-lobe of HLf¹. The Cys157 is involved in S-S bond formation with the Cys173¹. From the available crystal structure data, the 153-158 sequence stretch of HLf is found to adopt a β -strand and the stretch from 158 to 161 a β -turn¹. This unique octapeptide fragment FSASCVPG with a high sequence homology might be involved in the biological function of the protein.

The solid-phase synthesis and conformational analysis of the octapeptide fragment FSASCVPG by the combined use of 2D-NMR spectroscopy and restrained molecular dynamics are reported here. The dimethyl sulfoxide-d₆ (DMSO-d₆) is used as the solvent, because the peptide is highly soluble in the solvent and also the solvent exchange reaction of amide protons is absent in DMSO-d₆⁴. The experimental structure of this peptide has been compared with the reported structure of the corresponding fragments in HLf and other lactoferrins. Structure prediction of this sequence has also been carried out and the predicted structure has been compared with the experimental structures.

Materials and Methods

Synthesis of the octapeptide FSASCVPG

Chloromethylated (functional group capacity = 2 mM -Cl/g) 2% 1, 4-butanediol dimethacrylate cross-linked polystyrene (BDDMA-PS)⁵⁻⁸ was used for the synthesis of the octapeptide FSASCVPG. The side-chain protecting groups used on the tert-butyloxy carbonyl (Boc)-amino acids were benzyl ether (Ser) and acetamidomethyl (Cys). The peptide was assembled on the resin by manual solid phase method using Boc-amino acid strategy⁹. Dicyclohexyl carbodiimide (DCC)-mediated 1-hydroxybenzotriazole (HOBt) active ester coupling⁹ in N-methyl pyrrolidone medium was done. The cleavage mixture used was 90% trifluoroacetic acid (TFA)/5% thioanisole/5% ethanedithiol (EDT). The crude sample was purified with FPLC (AKTA, Amersham Biosciences) using Superdex peptide HR 10/30 column and solvent system 0.1% trifluoroacetic acid

(TFA, solvent A) and 0.1% TFA in 80% acetonitrile (solvent B).

Nuclear magnetic resonance

About 8 mg of purified peptide was dissolved in 0.6 ml of DMSO-d₆. All the ¹H-NMR spectra on the peptide were recorded on a Varian Unity⁺ 600 MHz spectrometer. The temperature coefficients for ¹H^N shifts were measured from the 1D ¹H-NMR spectra recorded at temperatures 293, 298, 303, 313 and 323 K. The 2D spectra included a set of 2D rotating-frame Overhauser enhancement spectroscopy (2D ROESY)^{10,11} with mixing time 500 ms, a double-quantum filtered correlation spectroscopy (2D DQF-COSY)¹² and total correlation spectroscopy (2D TOCSY)¹³⁻¹⁵ with mixing period of 75 ms. A temperature of 25°C was used in all the experiments. In 2D experiments, time domain data points were 512 and 2048 along t₁ and t₂ dimensions, respectively. The data multiplied with sine bell window functions shifted by $\pi/4$ and $\pi/8$ along t₁ and t₂ axes, respectively, was zero-filled to 1024 data points along t₁ dimensions prior to 2D-fourier transform. ¹H chemical shift calibrations were carried out with respect to the methyl signal (at 0.0 ppm) of 3-(trimethylsilyl) [3,3,2,2-²H] propionate-d₄ (TSP), which was used as an external reference.

Modeling by restrained molecular dynamics was performed by using the software package CYANA¹⁶. Ten thousand torsional angle dynamics steps were performed with a simulated annealing procedure on each of the 1000 initially generated structures. The structures were visualized and analyzed using the software package MOLMOL¹⁷.

Results and Discussion

Peptide synthesis

The 2% cross-linked BDDMA-PS was found to be an efficient polymer support for peptide synthesis. The functional group capacity of the resin was 2 mM -Cl/g. Attachment of the first amino acid (Gly) was nearly quantitative (1.8 mM -NH₂/g). Single step coupling, with 3 mM excess of the reagents, was required for each monomer for completion. The yield

	1	10	140	153	160	170	670	691		
BLF	APRKNVRWCT	-----	ESLEPFQGA	VF	FSASCVPC	VD	DRQAYPNLC	-----	AIANLKKCSTSP	PLLEACAFLTR
CLF	APRKNVRWCT	-----	ESLEPLQGA	VF	FSASCVPC	ID	RQAYPNLC	-----	AIANLKKCSTSP	PLLEACAFLTR
GLF	APRKNVRWCA	-----	ESAELQGA	VF	FSASCVPC	VD	GKAYPNLC	-----	AIANLKKCSTSP	PLLEACAFLTR
PLF	APKGVWRVCV	-----	GPPEPLQKA	VF	FSQSCVPC	CA	DGNAYPNLC	-----	AIAT	
MLF	APRKSVRWCT	-----	GPPEPLQKA	VF	FSASCVPC	CA	DGKQYPNLC	-----	SITNLRRCSS	SPLEACAFTRA
HLF	GRRRSVQWCA	-----	GPPEPIEA	VF	FSASCVPC	AD	GKQFPNLC	-----	GITNLRRCSTSP	PLLEACEFLTR

Fig. 1—Octapeptide FSASCVPG that forms highly conserved region (shown in bold) in various lactoferrins²

was 93% (53 mg peptide from 100 mg of peptidyl resin). A major single peak in the chromatogram indicated high purity. The peptide was characterized by the sequential ^1H resonance assignment of all amino acid residues using 2D ^1H NMR spectra.

NMR analysis

Sequence-specific resonance assignments

Complete sequence-specific ^1H -NMR assignments of the octapeptide were achieved as described previously¹⁸. As a first step in this direction, amino acid residues in the octapeptide were classified on the basis of their side chain spin systems and identified¹⁸. The Gly residue could be identified on the basis of its H^α - H^β connectivity pattern in the 2D DQF-COSY spectrum. Pro was identified using correlations to the C_αH and C_βH signals in the 2D TOCSY spectrum. The amino acids Ser, Phe and Cys belong to the AMX spin system. There were four AMX spin systems (2 Ser, 1 Phe and 1 Cys). Identification of all 4 pairs of H^α - H^β connectivities was straightforward with the combined use of 2D DQF-COSY and TOCSY. Downfield shifts of both H^β protons in the case of Ser residues helped in distinguishing them from other AMX spin systems. The two Ser residues were distinguished from their sequential NOE connectivities to their neighbours. Ser-4 showed $d_{\alpha\text{N}}$ connectivity to Cys-5, while Ser-2 showed $d_{\alpha\text{N}}$ connectivity to Ala-3. The aromatic AMX spin system, Phe, was identified from the observation of NOEs from the H^β protons to the nearest aromatic ring protons in the 2D ROESY spectrum. The Ala and Val could be assigned from their characteristic connectivity pattern in 2D TOCSY. Ala showed characteristic methyl to H^α connectivity. In Val, two methyl groups were connected to H^β , which in turn was connected to H^α . Once, the side chain protons were identified the backbone $^1\text{H}^\text{N}$ protons were attached to the respective H^α proton resonances using 2D NOE and 2D TOCSY spectra. As an illustration of this, Fig. 2 shows the fingerprint (H^N - H^α) region of the 2D TOCSY spectrum.

Once the respective ^1H resonances were identified as belonging to specific amino acid residues present in the octapeptide, nOes in 2D NOESY spectrum were used for sequence-specific resonance assignments. However, nOes are a function of the rotational correlation time (τ_c), varying from -1 at large τ_c to 0.5 at low τ_c , for relaxation via ^1H - ^1H dipolar interactions. For the octapeptide under investigation, the absence of sequential nOes even in

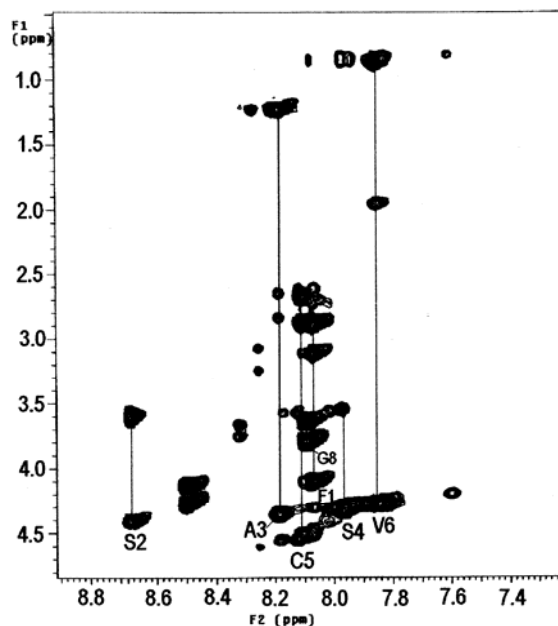


Fig. 2— H^N -aliphatic region of TOCSY of FSASCVPG in DMSO-d_6

the long mixing time (500 ms) 2D NOESY spectrum indicated that the τ_c of octapeptide was close to the cross-over point in the relationship between τ_c and nOe. It was thus necessary to obtain nOes from 2D ROESY spectra, as they were always positive in this spectrum.

The cross-peaks observed in the 2D ROESY spectra helped in complete sequential assignments. Sequence-specific resonance assignment, using 2D ROESY spectrum was started from the N-terminal Phe residue. The nOe cross-peaks corresponding to sequential distance $d_{\alpha\text{N}}$ led to the sequence-specific ^1H resonance assignments of all the residues. We could walk all along the backbone of the polypeptide chain monitoring $d_{\alpha\text{N}}$ nOe connectivities, except between Val-6 and Pro-7, since Pro-7 had no H^N proton. The nOe observed between H^β protons of Pro-7 and H^α of Val-6 helped in assigning the Val-6-Pro-7 stretch. As an illustration of this, Fig. 3 shows the fingerprint (H^N - H^α) region of the ROESY spectrum recorded with a mixing time of 500 ms. Such assignment was further supported by observation of sequential H^N - H^N connectivities (Fig. 4).

The presence of few additional short-range nOes and the absence of any long-range nOes in the ROESY spectrum indicated the lack of a persistent secondary structure (α -helix or β -sheet). The cross-peak intensities obtained in the 2D ROESY spectrum

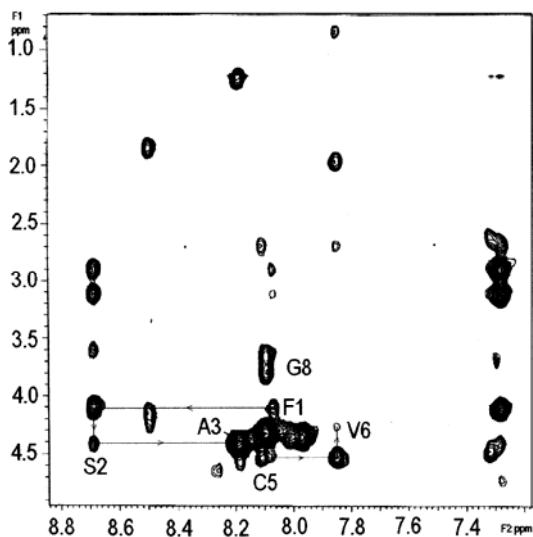


Fig. 3— H^N -aliphatic region of ROESY of FSASCVPG with mixing time 500 ms in $DMSO-d_6$

Table 1—Observed 1H NMR chemical shifts of FSASCVPG in $DMSO-d_6$

Residue	H^N	H^a	H^b	Others
F1	8.07	4.11	2.89, 3.12	Aromatic 2,6H 7.30 4H 7.27 3,5 H 7.19
S2	8.69	4.40	3.56, 3.61	
A3	8.19	4.35	1.23	
S4	7.97	4.32	3.54, 3.66	
C5	8.11	4.56	2.68, 2.89	
V6	7.85	4.27	1.95	γ CH3 0.84, 0.89
P7		4.36	2.02, 1.91	γ H 1.83 δ H 3.56, 3.67
G8	8.09	3.64, 3.80		

were translated into distance constraints. The NOE cross-peak intensities were classified as strong ($<2.5 \text{ \AA}$), medium ($2.5 \text{ \AA} < x < 3.5 \text{ \AA}$) and weak ($>3.5 \text{ \AA}$).

The observed chemical shift values are given in Table 1. Examination of chemical shifts of a peptide could provide indications about secondary structure^{19,20}. The chemical shift index developed by Wishart *et al.*²⁰ involved comparing α -proton chemical shifts to random coil chemical shifts and α -helices or β -sheets could be identified by characteristic patterns of this index. Residues belonged to α -helices showed a high field shift in their H^a chemical shifts, while those belonged to β -

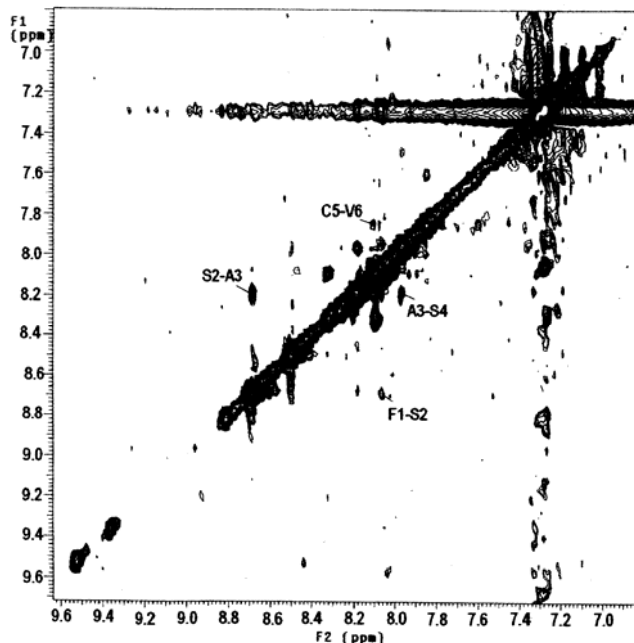


Fig. 4— H^N - H^N region of ROESY of FSASCVPG with mixing time 500 ms in $DMSO-d_6$

Table 2— $^3J_{NH\alpha}$, ϕ and $-\Delta\delta/\Delta T$ of H^N protons of FSASCVPG in $DMSO-d_6$

Residue	$^3J_{NH\alpha}$ (Hz)	ϕ ($^\circ$)	$-\Delta\delta/\Delta T$ (ppb/K)
F1			-1.12
S2	7.80	-148	-4.65
A3	7.49	-161	-4.70
S4	7.61	-156	-4.41
C5	7.85	-151	-4.64
V6	8.50	-141	-4.0
P7			
G8	5.03	-176	-5.53

strands/sheets showed a low field shift in their H^a chemical shifts. An uninterrupted set of four or more +ve or -ve values usually taken as an indication of a β -sheet or α -helix respectively²⁰. The chemical shift index (CSI) values of the octapeptide FSASCVPG, Phe (-1), Ser (0), Ala (0), Ser (-1), Cys (0), Val (-1), Pro (0) and Gly (-1, -1) did not meet criteria for either of β -sheet or α -helix.

Temperature dependence of amide proton resonances

In peptide NMR, the chemical shifts of amide proton resonances displayed temperature dependence²¹. The value of the amide proton temperature coefficient has been widely used to predict hydrogen bond donors²²⁻²⁵. The values more positive than about -3 ppb/K indicate that the amide

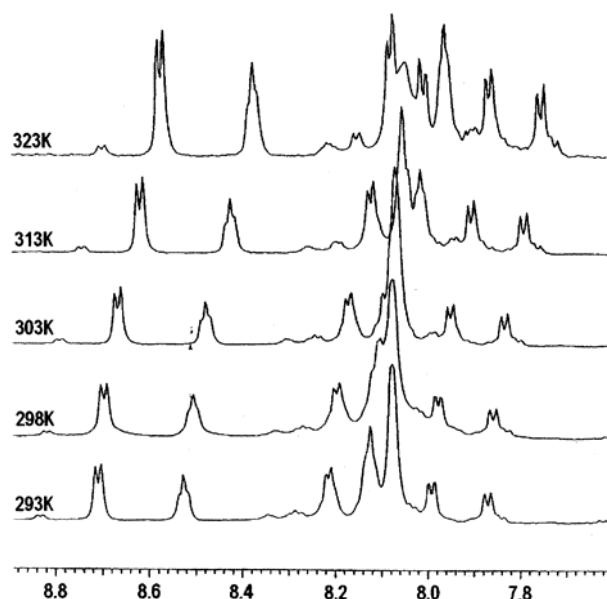


Fig. 5—Temperature-dependent 1D ^1H NMR spectra of FSASCVPG in DMSO-d_6

proton is involved in intramolecular hydrogen bonding²⁶. From the temperature coefficients of amide protons (Table 2) of the octapeptide FSASCVPG, it was clear that no amide proton (H^{N}) was involved in hydrogen bonding. The temperature-dependent 1D ^1H -NMR spectrum is given in Fig. 5.

$^3J_{\text{NH}\alpha}$ Coupling constants

The $^3J_{\text{NH}\alpha}$ coupling constant is a function of the dihedral angle ϕ and can be used to identify different peptide conformations¹⁸. The possible ϕ torsional angles were calculated from $^3J_{\text{NH}\alpha}$ values using the Karplus-type equation^{27,28}. The observed $^3J_{\text{NH}\alpha}$ coupling constants and ϕ values for the octapeptide are given in Table 2. All the $^3J_{\text{NH}\alpha}$ coupling constants for the octapeptide were higher than 7.0 Hz and were characteristic of a predominantly extended backbone conformation²⁸.

3D Structure calculation

Restrained molecular modeling was performed by running molecular dynamics simulations based on the torsional angle dynamics (TAD) approach as implemented in the CYANA package¹⁶. Dipolar connectivities were quantitated in 2D ROESY spectrum. Overall, 57 meaningful upper limit distance restraints could be collected. These were complemented with six ϕ torsion angle restraints. The ϕ values were obtained by assessment of local secondary structure from the set of $^3J_{\text{NH}\alpha}$ coupling

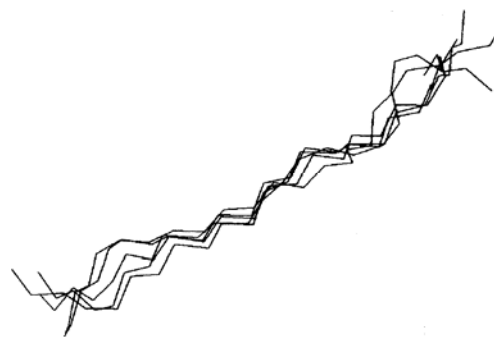


Fig. 6—Best-fit backbone superposition for the lowest target function subset of 5 conformers resulting from NMR-restrained molecular dynamics calculations of FSASCVPG with CYANA

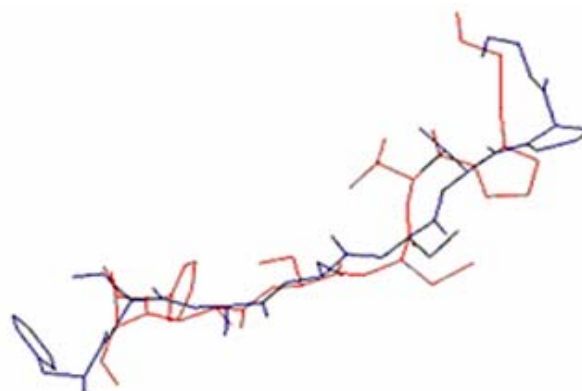


Fig. 7—Superposition of calculated structure of FSASCVPG with lowest target function (blue) on reported structure of the corresponding protein fragment (red)

constants. Out of the 1000 random conformers selected for molecular dynamic simulations, the 20 structures with the lowest global deviation (minimum target function) from the input restraints were sorted out and submitted to statistical analysis. Backbone best-fit superposition of the 5 conformers is shown in Fig. 6. The mean global backbone RMSD was 0.981 Å.

Overall, the octapeptide FSASCVPG had a predominantly extended backbone conformation (β -strand like) in DMSO-d_6 at 25°C. The nOe observed between H^{δ} of Pro-7 and H^{α} of Val-6 fixed the His-6-Pro-7 peptide bond in the trans configuration. The calculated structure with the least target function was superimposed on the reported structure of the corresponding protein fragment¹. It showed a superposition (Fig. 7) with a mean global backbone RMSD of 1.78 Å. The solved structure resembled closely to the reported structure of the corresponding

protein fragment. The calculated and reported structures of different lactoferrins such as MLf, GLf, CLf, BLf, PLf and HLf were superimposed in a pairwise manner (mean global backbone RMSD < 1.9 Å). Since, the RMSD was less than 1.9 Å, we could understand that all segments had almost similar 3D structures and might have some biological significance.

Structure prediction with advanced protein secondary structure prediction (APSSP)²⁹ algorithm showed that the peptide adopted a random coil structure. This might be due to the lack of long-range forces that make the major contribution to the folded state of proteins. The APSSP method is a combination method for protein secondary structure prediction based on neural network and example-based learning²⁹.

Conclusion

The 2% 1, 4-butanediol dimethacrylate cross-linked polystyrene (BDDMA-PS) is an efficient polymer support for the synthesis of oligopeptides. NMR analysis and restrained molecular dynamics showed that the octapeptide FSASCVPG had a predominantly extended backbone conformation in DMSO-d₆ at 25°C. The calculated structure resembled closely to the reported local structure of the corresponding HLf protein fragment. The predicted structure did not match with the experimental structure. This might be due to the lack of long-range forces that make the major contribution to the folded state of proteins. Since the RMSD between the calculated and reported local structures of different lactoferrins was less than 1.9 Å, the all segments were assumed to have almost similar 3D structures.

Acknowledgement

We acknowledge the facilities provided by the National Facility for High Field NMR located at TIFR, Mumbai and supported by DST. Department of Science and Technology, Government of India is gratefully acknowledged for their financial assistance.

References

- 1 Haridas M, Anderson B F & Baker E N (1995) *Acta Cryst Sect D* 51, 629-646
- 2 Viejo-Diaz M, Andres M T, Perez-Gil J, Sanchez M & Fierro J F (2003) *Biochemistry (Moscow)* 68, 217-227
- 3 Karthikeyan S, Sharma S, Sharma A K, Paramasivam M, Yadav S, Srinivasan A & Singh T P (1999) *Curr Sci* 77, 241-255
- 4 Christopher Jones, Barbara Mulloy & Adrian H T (eds.) (1993) *Methods in Molecular Biology-Spectroscopic Methods and Analysis*, Vol. 17, pp. 117-126
- 5 Roice M, Kumar K S & Pillai V N R (2000) *Tetrahedron* 56, 3725-3734.
- 6 Roice M, Kumar K S & Pillai V N R (1999) *Macromolecules* 132, 8807-8815.
- 7 Ajikumar P K & Devaky K S (2000) *Lett Pept Sci* 7, 207-215.
- 8 Sunil Kumar P N, Devaky K S, Sadasivan C & Haridas M (2002) *Prot Pept Lett* 9(5), 403-409
- 9 Stewart J M & Young J D (1984) *Solid Phase Peptide Synthesis*, Vol. 2, pp.71-86, Pierce Chemical Co., Rockford, IL
- 10 Bax A & Davis D G (1985) *J Magn Reson* 63, 207-213
- 11 Bothner-By A A, Stephens R L, Lee J, Warren C D & Jeanloz R W (1984) *J Am Chem Soc* 106, 811-813
- 12 Piantini U, Sorensen O W & Ernst R R (1982) *J Am Chem Soc* 104, 6800-6801
- 13 Bax A & Davis D G (1985) *J Magn Reson* 65, 355-360
- 14 Braunschweiler L & Ernst R R (1983) *J Magn Reson* 53, 521-528
- 15 Bax A & Davis D G (1985) *J Am Chem Soc* 107, 2820-2821
- 16 Güntert P, Mumenthaler C & Wüthrich K (1997) *J Mol Biol* 273, 283-298
- 17 Koradi R, Billeter M & Wüthrich K (1996) *J Mol Graphics* 14, 51-55
- 18 Wüthrich K (1986) *NMR of proteins and Nucleic Acids*, pp. 54-155, Wiley Interscience, New York
- 19 Pastore A & Saudek V (1990) *J Magn Reson* 90, 165-176
- 20 Wishart D S, Sykes B D & Richards F M (1992) *Biochemistry* 31, 1647-1651
- 21 Ohnishi M & Urry D W (1969) *Biochem Biophys Res Commun* 36, 194-202
- 22 Jimenez M A, Nieto J L, Rico M, Santoro J, Herranz J & Bermejo F J (1986) *J Mol Struct* 143, 435-438
- 23 Dyson H J, Rance M, Houghten R A, Lerner R A & Wright P E (1988) *J Mol Biol* 201, 161-200
- 24 Andersen N H, Chen C, Marschner T M, Krystek Jr S R & Bassolino D A (1992) *Biochemistry* 31, 1280-1295
- 25 Skaliky J J, Selsted M E & Pardi A (1994) *Proteins* 20, 52-67
- 26 Kople K D, Ohnishi M & Go A (1969) *J Am Chem Soc*, 91, 4246-4251
- 27 Karplus M (1963) *J Am Chem Soc* 85, 2870-2876
- 28 Bystrov V F (1976) *Prog Nucl Magn Reson Spectrosc* 10, 41-81
- 29 Raghava G P S (2000) *Protein secondary structure prediction using nearest neighbour and neural network approach, CASP4*, 75-76